Acta Crystallographica Section D
Biological Crystallography
ISSN 0907-4449

Matching X-ray source, optics and detectors to protein crystallography requirements

Colin Nave

CCLRC Daresbury Laboratory, Daresbury Warrington WA4 4AD, England

Correspondence e-mail: c.nave@dl.ac.uk

Received 5 February 1999
Accepted 22 June 1999

A review of the requirements for collecting X-ray diffraction data from protein crystals is given, with an emphasis on the properties of the crystal and its diffraction pattern. The size, unit-cell dimensions and perfection of the crystals can all be related to the required size and divergence of the incident X-ray beam, together with the size and spatial resolution of the detector. The X-ray beam causes primary radiation damage, even in frozen crystals. If the incident beam is very intense, temperature rises and gradients could occur in the crystal. The extent to which these problems can be overcome is also discussed.

1. Introduction

X-ray diffraction patterns from protein crystals were obtained over 60 years ago using what were by modern standards low-intensity X-ray sources. Since then, there have been many developments in instrumentation, including brighter X-ray generators, synchrotron-radiation sources, focusing optics and electronic detectors. Protein crystallographic projects are now being pursued for their scientific importance rather than their technical feasibility. As a result, small poorly diffracting crystals are now becoming the norm and the requirements for protein crystallography are increasingly driving many of the developments. This article reviews the instrumentation requirements for collecting X-ray diffraction data from a protein crystal, with emphasis on the properties of the crystal and its diffraction pattern. Parameters such as the wavelength, intensity, size and divergence of the X-ray beam and the size and resolution of the detector can all, in principle, be derived from the properties of the protein crystal. These considerations apply to use of both conventional X-ray generators and synchrotron-radiation sources.

2. Properties of the sample and its diffraction pattern

The obvious properties of a protein crystal are its dimensions, unit-cell size and perfection. The type and content of solvent are not covered here, but it should be noted that the solvent can affect the susceptibility to radiation damage and the ability to successfully freeze the crystal to cryo-temperatures.

A very simple mosaic block model (Fig. 1) for crystal imperfections was described by Nave (1998*a*) following on from the work of Helliwell (1992). The three parameters used to describe the properties of the mosaic block model were the angular distribution of the mosaic blocks, the size of the mosaic blocks and the variation in unit-cell dimensions between (or within) mosaic blocks. Each of these parameters can affect the rocking width of any Bragg reflection and the angular divergence of the diffracted X-ray beam.

There have been several examinations of the perfection of protein crystals and it is undoubtedly true that highly perfect crystals can be obtained (Colapietro *et al.*, 1992; Fourme *et al.*, 1995; Snell *et al.*, 1995; Stojanoff *et al.*, 1997). Rocking widths for individual reflections as low as 0.002° have been measured. However, data collection is increasingly being carried out from protein crystals at cryo-temperatures. Present cryo-procedures mean that it is difficult to retain a high degree of perfection in the protein crystal, and rocking widths of 0.1° appear to be the best which can be obtained. A review of freezing procedures and the effects on the crystal can be found in Garman & Schneider (1997). An examination of diffraction patters from a frozen crystal of lysozyme showed that, in this case, the dominant imperfection was the variation in unit-cell dimensions (Nave, 1998*b*). A variation in unit-cell dimensions of just 0.2% would lead to a rocking width of 2 mrad (∼0.1°). The effect on the angular width of the diffracted beam would vary with Bragg spacing d (= $\lambda/2\sin\theta$). For the above case, at 1 Å wavelength and d = 2 Å the angular width of the diffracted beam would increase to 0.05°. For d = 1 Å it would increase to 0.1°.

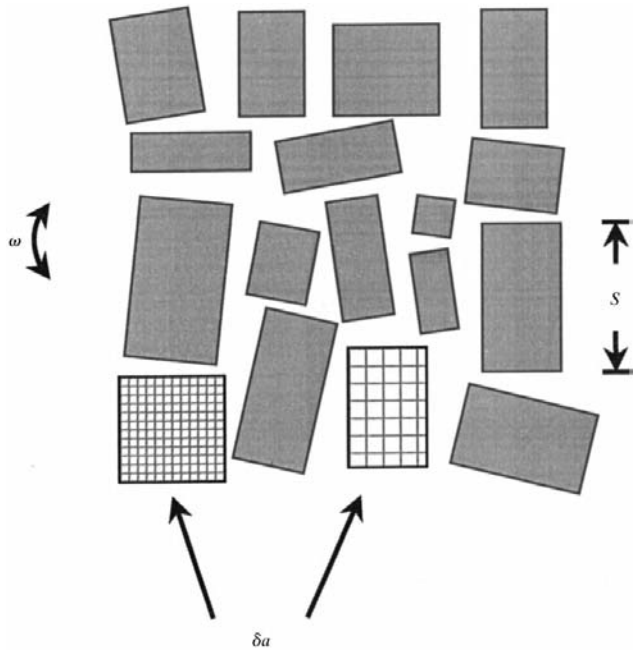

Figure 1
A mosaic block model of a crystal showing a spread in the orientation ω of the mosaic blocks, a spread in the size s of the blocks and a variation δa in the unit-cell dimensions between different blocks.

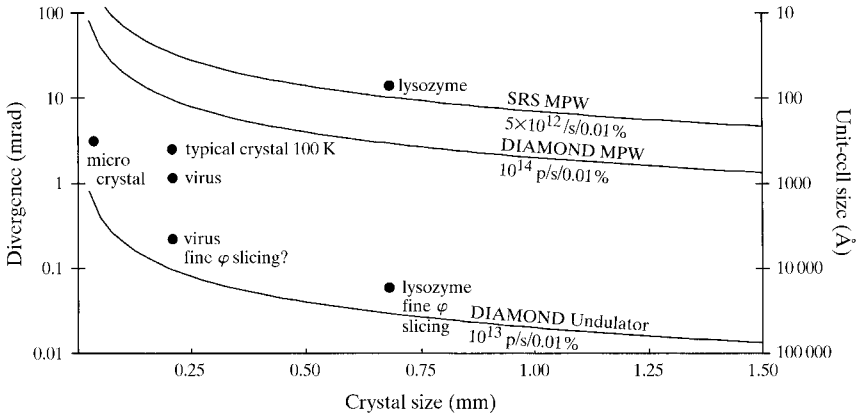

Figure 2
Size–divergence diagram for X-ray scattering. The horizontal axis represents the size of the specimens to be studied and the required divergence of the beam is shown on the left-hand vertical axis. The right-hand axis gives the corresponding unit-cell dimension. This would be on the limit of being resolved with an X-ray beam of this divergence using 1 Å radiation. Three sources are shown as curved lines having emittances of 7, 2 and 0.02 mm mrad. These are based on FWHM (2.35σ) values for the beam size and divergence. The flux from these sources in a 0.01% bandpass (as given by a crystal monochromator) is shown. This diagram is, therefore, a slice at a bandpass of 0.01% through the three-dimensional size–divergence–bandpass diagram. Filled circles represent the requirements for some representative samples or experiments. Fine φ slicing refers to the case where one is collecting data in fine rotation increments and the incident beam divergence matches the crystal perfection.

3. Matching the size and divergence of the X-ray source to the requirements

Various considerations relating to the matching of X-ray sources to experimental requirements for diffraction are given in Rosenbaum & Holmes (1980). These considerations are not confined to data collection using synchrotron-radiation sources. Very highly collimated beams can also be obtained from X-ray tubes. The principles of obtaining these beams are described for a synchrotron by Lindley (1999) and for X-ray tubes by Arndt (1990), Bloomer & Arndt (1999) and Yang *et al.* (1999). A graphical way of illustrating the way an X-ray source can be matched to the experimental requirements is given in Nave (1998*a*). An example, for the case of protein crystallography, is given in Fig. 2. The position of any sample on the diagram is given by its size, together with its unit-cell dimensions (if the aim is simply to resolve the diffraction orders) or perfection (if the aim is to match the crystal perfection). Ideally, the X-ray beam should be the same size as the sample. A smaller beam would result in increased radiation damage during data collection, while a larger beam would result in increased background. The divergence of the X-ray beam should ideally be less than the reflection rocking width or diffracted beam divergence from the crystal. However, it is common to collect data with larger rotation ranges of the crystal in order to minimize the number of images required. The beam divergence still has to be suffi-

ciently small to resolve the largest unit-cell dimension in the crystal.

Focusing monochromators can be used to alter the size, divergence and wavelength spread of the beam in more complex ways. This would require an extra dimension (wavelength spread) to be added to Fig. 2. A description of the way focusing elements and monochromators transform the properties of the X-ray beam has been given in Matsushita & Kaminaga (1980*a*,*b*).

Fig. 2 also shows the X-ray flux which could be delivered by some typical synchrotron X-ray sources. In order to match each source to the requirements of the specimen, focusing optics can be used. These can, for example, demagnify the source at the expense of increased divergence. This procedure is equivalent to moving along the lines of constant emittance shown for each source. An alternative is to decrease the size or divergence of the X-ray beam (at the expense of flux) using slits or collimators. The multipole wiggler source has 100 times the emittance of the undulator, but it also has approximately ten times the flux. Its performance should, therefore, be better than the undulator for undemanding applications. However, the multipole wiggler has a total power output of up to 20 kW, and the resulting heat-load problems on the beamline makes it extremely difficult to realise the full potential of these devices. The superior ratio of useful photon flux to total flux is one of the reasons why undulators are such good sources for protein crystallography.

4. Detector requirements

The availability of reliable electronic detectors has revolutionized data collection for protein crystallography, with image-plate and CCD-based systems now the most widely used. These systems have been developed for protein crystallography and, as a result, match the requirements quite well. However, some further improvements in the performance of the detectors would still give significant advantages for some applications.

The detectors need to have a suitable spatial resolution and size to resolve all the features on the diffraction pattern. In general, the CCD systems have a smaller size but better spatial resolution than the image-plate systems. The CCD-based systems are matched to the case where the diffraction features are sharp; for example, where small-size beams are being used to study small crystals. The CCD systems generally also have a shorter read-out time than the image-plate systems and are, therefore, well matched to powerful synchrotron-radiation sources, although the short read-out times can also be of benefit on a conventional X-ray source (Muchmore, 1999).

The detectors should also be able to record the data efficiently with near photon-counting statistics. The efficiency is expressed as the DQE (detector quantum efficiency) of the system, which compares the statistics obtained from the detector with the intrinsic photon statistics in the diffraction pattern. A useful way of expressing the DQE is as a function of the incident photon flux over an area the size of a Bragg spot (*e.g.* Stanton *et al.*, 1992). Many detector systems have a DQE over 0.5 for a wide range of intensities, with the DQE falling significantly for intensities less than a few hundred photons per spot. This is not a limitation for the normal case, where the statistics are limited by the X-ray background from the specimen rather than the detector noise.

The X-ray background can be improved in two ways: by recording the data in fine rotation increments (fine φ slicing) or by placing a larger detector further away. The intention in both cases is to minimize the range over which background is being recorded. Both strategies require the diffraction spot to occupy a small volume of reciprocal space. By defining the volume of the spot in reciprocal space, one can define the intrinsic signal-to-background ratio for a particular crystal. It should then be possible to define how far one can go in reducing the background using fine φ slicing or large detectors.

As an example, for a crystal at cryo-temperatures, a rocking width of 0.1° and a beam divergence (1 Å wavelength and 2 Å resolution) of 0.05° might be obtained. The spatial resolution obtainable from image-plate detector systems is approximately 0.6 mm. The divergent diffracted beam would increase to this value and therefore match the detector resolution for a detector placed 500 mm away. To record the data at 2 Å resolution would then require a detector of 550 mm in diameter centred on the incident beam. (Note that if the diffracted beam divergence is a consequence of a variation in unit-cell dimensions, the maximum useful detector size would, to a first approximation, be independent of the resolution of the data.) The increase in area over a 350 mm detector would give a factor of 2.5 improvement in the peak-to-background ratio. By collecting data at 0.1° φ slices rather than 1° slices, a further factor of ten improvement could be obtained in principle, giving a factor of 25 in all. The conclusion is that for the best-ordered samples at cryo and room temperatures, a significant improvement in the peak-to-background ratio could be obtained. In some cases, the statistics might then be limited by the detector noise rather than the X-ray background.

A discussion of the benefits and pitfalls of fine φ-slicing techniques can be found in Pflugrath (1999). If one is collecting data in fine φ slices, a detector with a fast read out is necessary in order to maintain a reasonably high-duty cycle. Most image-plate systems have a read-out time which is too long for fine φ slicing on a synchrotron source, although they could be used in this mode on a conventional X-ray source. CCD systems have a shorter read-out time (often a few seconds), but a compromise has to be made between the read-out time and the read-out noise. This compromise could eventually limit the applicability of CCD systems for data collection in fine φ-slicing mode. Multiwire proportional counters have a very fast read-out time and a low noise, but have a limited count-rate capabilities. The benefits of the low noise and fine φ-slicing capability has been illustrated by Kahn & Fourme (1996).

The above argument applies to the case where one is collecting data at the limit of the resolution from the crystal. In these cases, an unfavourable peak-to-background ratio will generally be present. For heavy-atom substitution and

anomalous scattering applications, one would want the best possible statistics for the medium to strong data which contributes most to the electron-density map. Accurate recording of the weak data is also required, as this is used to solve the structure of the heavy atoms or anomalous scatterers. Anomalous scattering applications, therefore, require a detector with a high DQE over a wide dynamic range.

For the most demanding time-resolved applications, the requirement is to record the data as quickly as possible. The instantaneous intensity on the detector will generally be very high, but the integrated intensity in each frame will be quite low owing to the short exposure time. Either a very fast photon-counting system (to cope with the high instantaneous rate) or an integrating detector with a high DQE for weak signals (to measure the weak data) is required.

The conclusion of the above is that further improvements in detector technology could usefully be made. Reduction in the dead-time of integrating detectors and increased detector area are obvious areas for improvement. Detectors with lower dark noise could be useful for some applications. For the future, a large number of groups are now developing photon-counting or integrating pixel detectors, in which each element has its own processing electronics. It is possible that these will be the detectors of choice in a few years time.

5. Wavelength requirements

In a diffraction experiment, one wants to maximize the elastic (Rayleigh) scattering and minimize interactions which result in deposition of energy in the sample. A discussion on the relative cross sections for Rayleigh scattering and photoelectric absorption is given in Arndt (1984). It was concluded that there would be benefit in going to much shorter wavelengths if radiation damage depended on the number of absorbed photons, but little benefit if it depended on the amount of absorbed energy. With the contribution of Compton scattering, the total deposited energy per scattered photon (in a defined resolution range) is actually predicted to increase as the wavelength of the photon is reduced (Nave, 1995). There are interesting discussions on this subject in Henderson (1995) and Sayre & Chapman (1995).

Anecdotal evidence indicates that, for some samples at room temperature, less radiation damage occurs at 0.9 Å wavelength compared with 1.5 Å wavelength. It is possible that this observation arises from effects such as increasing thermal gradients and loss of scattered photons owing to absorption at the longer wavelengths. Very few systematic studies have been carried out in this area. An examination of radiation damage for a crystal at cryo-temperatures using attenuated white beams was carried out by Gonzalez & Nave (1994). Different wavelength profiles in the incident beam were used and the radiation damage appeared to follow the energy absorbed rather than the number of photons absorbed. However, this investigation was not carried out with the purpose of investigating wavelength-dependent effects and cannot be regarded as definitive.

Although one moves the detector further away at shorter wavelengths, the background is not reduced, as it mainly arises from an elastic scattering process. The background is concentrated into a smaller range of angles at shorter wavelength in a way which approximately compensates for the increased detector distance (Gonzalez *et al.*, 1994).

Longer wavelengths scatter more strongly but lead to increased absorption errors for larger samples. A discussion of these factors is given in Polikarpov *et al.* (1997). Collecting data at wavelengths around 0.9 Å means that one is on the favourable side of the absorption edge of many common heavy-atom derivatives. These considerations have led to an increased use of wavelengths under 1 Å for data collection. It is certainly possible to collect very good data for very short wavelengths (Schiltz *et al.*, 1997) and there seems to be no reason why absorption edges such as xenon and iodine *K* edges should not be exploited on higher energy synchrotron sources. Data collection at longer wavelengths (above 2 Å) is more problematic owing to increased absorption effects. This will probably limit the exploitation of sulfur and phosphorous *K* edges and many *L* edges, despite the very large anomalous signals which can be obtained. A table showing the most common absorption edges for MAD analysis of protein structures is given in Ogata (1998).

The intrinsic wavelength bandpass given by monochromator systems based on perfect single crystals of semiconductors is approximately 10^{-4}. This is unnecessarily fine for many diffraction applications. The wavelength bandpass of the incident beam also increases the angular divergence of the diffracted beams. To match the angular broadening arising from other effects, the wavelength bandpass is given by $\delta\lambda/\lambda = \delta\theta\cot\theta$, where $\delta\theta$ is the angular divergence and θ is the Bragg angle. For the case considered above, with a 0.05° divergence at 2 Å resolution, the wavelength bandpass to match the divergence would be 3.4×10^{-3}. Note that if the divergence of the diffracted beam is a consequence of a variation in unit-cell dimensions, the required value of the wavelength bandpass would be approximately independent of resolution. The increase in $\delta\theta$ with resolution would be compensated by the change in $\cot\theta$.

For anomalous scattering applications, the required wavelength bandpass is defined by the natural width of the X-ray absorption edge and any near-edge features which can be exploited. A tabulation of the widths of various relevant X-ray absorption edges is given in Thompson (1997). The conclusion is that there is no great advantage in using an incident spectral bandpass of less than 10^{-4}. However, systematic experiments to verify this conclusion have yet to be carried out.

6. Intensity requirements

Higher intensity incident radiation will give greater intensity in the diffracted beams and, therefore, better statistics for a set exposure time. By this criteria, one would wish for the highest intensity possible. However, there are at least two factors which could limit the application of higher intensity beams.

Radiation damage occurs in all specimens after they have been subjected to a certain dose of X-rays. Primary radiation damage occurs when an X-ray is absorbed and produces a photo-electron. Compton scattering processes also deposit energy in the sample. Secondary damage occurs subsequently because of diffusion of free radicals or breakdown of the structural integrity of a crystal at room temperature. These secondary processes essentially cease at cryo-temperatures. However, the primary radiation-damage processes occur at both room temperature and cryo-temperature and it is difficult to see how they can be avoided. Henderson (1990) estimated that after an absorbed dose of 2×10^{17} keV mm^{-3}, significant radiation damage would occur in all specimens at cryo-temperatures. Experiments by Gonzalez & Nave (1994) were consistent with this prediction. For 1 Å radiation, this absorbed dose could occur in a matter of minutes on some undulator beamlines. These high intensities are necessary for time-resolved studies but cannot, for this reason, be fully exploited for obtaining accurate statistics from a single crystal, owing to radiation damage. Because of the fundamental physical nature of the primary radiation damage, it is unlikely that a very wide variation in the effect will occur for different specimens at cryo-temperatures.

A second effect which will occur at high intensities is a rise in temperature owing to the absorbed energy. An estimation of the temperature rises which could occur under adiabatic (no heat loss) conditions is given in Helliwell (1992). For undulator beamlines on a third-generation synchrotron source, temperature rises of several hundred degrees per second (incident intensity of 10^{15} photons sec^{-1} mm^{-2} at 1 Å wavelength) could occur. Heat will, of course, be emitted from the specimen as the temperature rises, particularly with the cryo-cooling methods which are now common. However, the analysis indicates that there will be a severe problem arising from temperature rises and temperature gradients in the crystal on very intense sources. Experience of these effects has been mainly anecdotal and there appears to have been difficulty in obtaining systematic data on the effects of very high incident intensity on protein crystals at cryo-temperatures. This is not suprising, as the effects will depend on the precise cooling regime adopted and parameters such as the surface-to-volume ratio, the specific heat and the thermal conductivity of the crystal. These last two effects will not only depend on the particular protein, mother liquor and cryo-protectants, but are also temperature dependent. It is, therefore, likely that the effects of temperature rise will be found to be more sample-dependent than the effects of primary radiation damage.

It should, however, be noted that as the incident beam hits a cooled crystal, it will create thermal gradients both along the path of the X-ray beam (owing to absorption effects) and transversely (if the beam is smaller than the crystal). Minimizing these effects by careful matching of crystal and beam dimensions could be of benefit in reducing heating effects.

There is also the possibility that relaxation processes can occur in a crystal. The relaxation processes could, in principle, restore the damaged area. At high incident intensity, multiple photon hits would not allow this relaxation to occur. If it occurred, this process would have a similar effect to that of beam heating – less data would be collected per crystal at high intensities.

The opposite effect could apply at extremely high intensities. The physical damage to a sample at high intensities takes place over many femtoseconds. If the intensity is sufficiently high, the data could be collected before the physical damage (*i.e.* the effects of the explosion!) appears. At even higher local photon fluxes, plasmas could form in attoseconds. This would destroy the diffraction pattern before it could be recorded. There might, therefore, be a window of high incident intensity where images and diffraction patterns could be recorded. This forms one of the arguments for developing the X-ray free-electron laser. A discussion of these possibilities can be found in Doniach (1996).

Finally, it should be noted that small intense X-ray beams could be exploited for collecting data from many individual small frozen crystals in a loop. The development of automatic methods of identifying each crystal and centring it in the X-ray beam would mean that such a procedure would be relatively painless, even if only one diffraction image could be obtained for each crystal.

7. Conclusions

To a large extent, the properties of the crystal (*e.g.* size, unit-cell dimensions) and its diffraction pattern (*e.g.* spot-to-background ratio, angular width of diffraction features) are intrinsic to the crystal. These properties exist independently of the properties of the radiation (*e.g.* size, divergence, wavelength spread) or detector (*e.g.* size, spatial resolution) used to record the data. The emphasis of this article has been on matching the properties of the X-ray beam and detector to the properties of the specimen. This approach should give the best possible data, whether working on a synchrotron or a home-based X-ray source.

References

Arndt, U. W. (1984). *J. Appl. Cryst.* **17**, 118.
Arndt, U. W. (1990). *J. Appl. Cryst.* **23**, 161–168.
Bloomer, A. C. & Arndt, U. W. (1999). *Acta Cryst.* D**55**, 1672–1680.
Colapietro, M., Cappuccio, G., Marciante, C., Pifferi, C., Spagna, R. & Helliwell, J. R. (1992). *J. Appl. Cryst.* **25**, 192–194.
Doniach, S. (1996). *J. Synchrotron Rad.* **3**, 260–267.
Fourme, R., Ducruix, A., Riès-Kautt, M. & Capelle, B. (1995). *J. Synchrotron Rad.* **2**, 136–142.
Garman, E. F. & Schneider, T. R. (1997). *J. Appl. Cryst.* **30**, 211–237.
Gonzalez, A., Denny, R. & Nave, C. (1994). *Acta Cryst.* D**50**, 276–282.
Gonzalez, A. & Nave, C. (1994). *Acta Cryst.* D**50**, 874–877.
Helliwell, J. R. (1992). *Macromolecular Crystallography with Synchrotron Radiation.* Cambridge University Press.
Henderson, R. (1990). *Proc. R. Soc. London Ser. B*, **241**, 6–8.
Henderson, R. (1995). *Quart. Rev. Biophys.* **28**, 171–193.
Kahn, R. & Fourme, R. (1996). *Methods Enzymol.* **276**, 268–286.
Lindley, P. (1999). *Acta Cryst.* D**55**, 1654–1662.
Matsushita, T & Kaminaga, K. J. (1980*a*). *J. Appl. Cryst.* **13**, 465–471.
Matsushita, T. & Kaminaga, K. J. (1980*b*). *J. Appl. Cryst.* **13**, 472–478.
Muchmore, S. (1999). *Acta Cryst.* D**55**, 1669–1671.
Nave, C. (1995). *Radiat. Phys. Chem.* **45**, 483–490.
Nave, C. (1998*a*). *J. Synchrotron Rad.* **5**, 645–647.

Nave, C. (1998*b*). *Acta Cryst.* D**54**, 848–853.
Ogata, C. M. (1998). *Nature Struct. Biol.* **5**, 638–640.
Pflugrath, J. (1999). *Acta Cryst.* D**55**, 1718–1725.
Polikarpov, I., Teplyakov, A. & Oliva, G. (1997). *Acta Cryst.* D**53**, 734–737.
Rosenbaum, G. & Holmes, K. C. (1980). *Synchrotron Radiation Research*, edited by H. Winick & S. Doniach, pp. 533–564. New York: Plenum Press.
Sayre, D. & Chapman, H. N. (1995). *Acta Cryst.* A**51**, 237–252.
Schiltz, M., Kvick, A., Svensson, O. S., Shepard, W., de la Fortelle, E., Prange, T., Kahn, R., Bricogne, G. & Fourme, R. (1997). *J. Synchrotron Rad.* **4**, 287–297.
Snell, E. H., Weisgerber, S., Helliwell, J. R., Weckert, E., Hölzer, K. & Schroer, K. (1995). *Acta Cryst.* D**51**, 1099–1102.
Stanton, M., Phillips, W., Li, Y. & Kalata, K. (1992). *J. Appl. Cryst.* **25**, 638–645.
Stojanoff, V., Siddons, D. P., Monaco, L. A., Vekilov, P. & Rosenberger, F. (1997). *Acta Cryst.* D**53**, 588–595.
Thompson, A. R. (1997). In *Proceedings of the CCP4 Study Weekend. Recent Advances in Phasing*, edited by K. R. Wilson, G. Davies, A. W. Aston & S. Bailey. Warrington: Daresbury Laboratory.
Yang, C., Courville, A. & Ferarra, J. (1999). *Acta Cryst.* D**55**, 1681–1689.